GÖRNERUP, M., HAYASHI, M., DÄCKER, C-.Å., and SEETHARAMAN, S. The non-destructive examination and alignment measurement of winder drum shafts in service. *VII International Conference on Molten Slags Fluxes and Salts*, The South African Institute of Mining and Metallurgy, 2004.

Mould fluxes in continuous casting of steel—characterization and performance tuning

M. GÖRNERUP*, M. HAYASHI*, C.-Å DÄCKER†, and S. SEETHARAMAN*
**Department of Materials Science and Engineering, Royal Institute of Technology, Stockholm, Sweden*
†Swedish Institute for Metals Research, Stockholm, Sweden

The mould flux plays a crucial role in the continuous casting operation of steel due to its multi-functional assignment as lubricator and heat flux controller. In reality, the commercial fluxes can fall short of the expectations of the operator. In such cases, the performance of the mould flux reduces production throughput in the casting machine.

This paper presents the results of a study of two different commercial mould fluxes in continuous casting of steels. The results of online sampling during casting, as well as off-line measurements in the laboratory, are presented. Mould flux powder and slag samples from the caster have been characterized with respect to melting behaviour, interfacial tension and thermal diffusivity, using various measuring techniques.

An experimental technique has been developed in order to simulate the melting behaviour of a flux in the mould, which has been found to be useful for qualitative studies. A cross-sectional view of different powders reveals that up to four different material layers may exist in the bed: a loosely packed powder layer, sintered layer, semi-solid layer and liquid slag layer.

It is found that the melting rate of the mould flux is dependent on the liquid slag layer thickness. Thus, in a continuous casting operation the melting rate is likely to be non-uniform with position in mould due to the difference in liquid slag layer thickness.

Mould slag composition is found to be influenced by the starting powder for as long as 30 min, representing a large part of the first heat casting time.

Observations of gas formation indicate that interfacial reactions between the steel and slag take place.

Keywords: continuous sacting, mould flux, mould slag, properties

Introduction

Although the mould flux function in continuous casting has been frequently discussed throughout the years, there are still some pieces of fundamental information missing in order to fully understand the different mechanisms controlling the different tasks of the mould flux during casting.

This paper discusses some of the phenomena observed during the first year of a 3-year project including both laboratory experiments and industrial trials. The work is part of a long-term project aimed at increasing the casting speed during the continuous casting of steel.

The mould flux in continuous casting

The mould flux functionality in continuous casting has been described elsewhere[1] and, thus, only a brief description will be given here, Figure 1.

During the casting operation, mould flux is continuously added to the top of the liquid steel, forming a layer with a total depth of 10–15 cm. Due to the high temperature of the liquid steel, well above the melting point of the flux, a temperature gradient forms in the vertical direction through the powder. On top is the newly added mould flux powder, forming a powder layer. Carbon and water are removed as the temperature rises and, at still higher temperatures, the

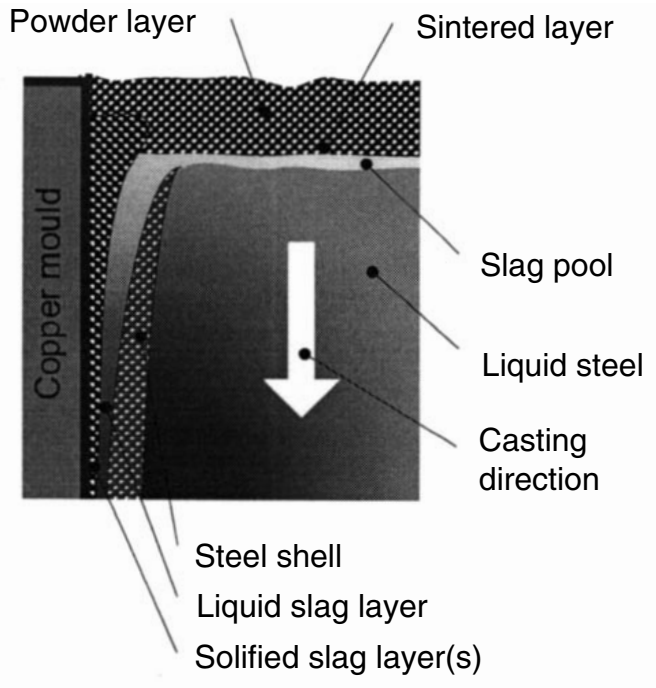

Figure 1. Schematic description of the mould flux powder bed, liquid pool, and solid layers in continuous casting

powder particles sinter together, forming a sintered layer. Liquid phases are formed in the lower part of the sintered layer and finally melting occurs. The liquid slag forms a pool on top of the steel melt inside the mould.

At the narrow and wide faces of the mould, the liquid slag penetrates the narrow gap between the steel meniscus and the mould wall. A solid, glassy slag layer is formed when liquid slag is quenched onto the water-cooled mould wall. If more slag is added onto this layer, or when preheating takes place, there is a likelihood of crystalline phases being formed in the layer. The solid slag layer structure is part of controlling the horizontal heat flux, i.e. the cooling rate of the steel, which directly relates to the number of surface defects occurring on the final product.

The temperature on the solid steel surface is above the melting point of the mould slag throughout the length of the mould. Consequently, a liquid slag layer is present between solid slag layers and the steel shell (strand). This layer is crucial to maintain a low strand/mould friction, thus avoiding sticking of the steel shell.

The functions of the mould flux constitute a task of great complexity, which can be summarized as follows:

- The top powder layer should effectively insulate the steel and ensure that no reoxidation takes place
- The liquid pool should have physical properties that promote the absorption of non-metallic inclusions, and avoid liquid slag entrapment into the liquid steel
- The liquid slag layer should be sufficiently thick in order to cover the whole top surface of the steel in the mould and, thus, ensure that liquid slag is continuously fed into the strand-mould wall gap at the meniscus
- The multi-layers between the strand and the mould wall should control the horizontal heat flux, i.e. the temperature and solidification rate of the steel shell
- The liquid slag layer between the mould and steel should stay liquid all through the mould length, i.e. fulfil the needs of mould lubrication.

Experimental work

Materials

In the present work two different commercial mould fluxes, used at two different steel plants, have been studied. The compositions and properties of these two powders are presented in Table I. The data presented are partly from the respective suppliers as well as the control stations in the steel plants.

The mould fluxes have been studied during operation, with sampling and measurement, and following characterization using laboratory techniques. In both plant study cases, the same starting powder has been used as presented in Table I.

It was sometimes necessary to pre-melt the mould flux powder before characterization in the laboratory equipment. This was done in a two-step method: (i) Decarburization of the powder in air at 800°C for 48 h, and (ii) melting in a Pt-crucible at high power input. The melting was either done in a vertical muffle furnace or by inductive heating, and the period of time at high temperature was kept to a minimum in order to minimize the evaporation of volatile components such as fluorides and alkalis from the mould flux liquid slag.

The liquid slag was quenched by pouring it onto a steel plate. The glassy slag obtained was either retrieved as pieces for further preparation before analyses or crushed and ground in a ball mill before further use.

Plant trials

The production trials took place at two different steel plants, both using slab casting machines but casting steel grades with significantly different chemical composition.

In plant A (mould flux A), a peritectic stainless steel grade was cast at 1500°C (temperature in tundish). The slab dimension was 1429 x 205 mm and the casting speed was 0.85 m/min. Four bags of starting powder, 5 kg each, were used before the production powder was added on top of the steel. The average mould flux consumption during the two-sequence casting was 1.0 kg/min (0.36 kg/m^2 slab surface).

In plant B (mould flux B), a low carbon steel grade for thin sheet production was cast in a two-heats sequence at 1532°C (temperature in tundish). The slab cross-section measured 1445 x 220 mm and 1525 x 220 mm for heat 1 and 2, respectively. Also in this case, 4 bags of starting powder were used. The casting speed was 1.35 m/min and the average powder consumption 1.45 kg/min (0.31 kg/m^2 slab surface).

During casting, samples of liquid slag were extracted from the mould for chemical analysis. This was done by lowering a 10 mm steel rod into the liquid slag pool at a position approximately 3/5 of the distance from the submerged entry nozzle (SEN) to the narrow face. The liquid slag attached itself onto the rod due to the cooling effect and could be extracted from the mould. The semi-solid slag was allowed to drip from the rod down onto a steel plate where solidification occurred instantaneously. The steel rod was again dipped into the slag pool and, by repeating this procedure numerous times, several grams of slag could be retrieved from the mould.

During the plant studies, all available operation parameters were logged using manual methods and available control system signals, e.g. cooling water flow and ΔT, casting speed, SEN depth, etc.

Table I
Mould flux compositions and properties

	Flux A	Flux B	Starting powder
Type:	Granulated	Granulated	-
Supplier data:			
%SiO_2	28.8	32.7	35.0–37.0
%CaO	36.5	28.8	37.5–39.5[A]
%MgO	1.3	1.77	
%Al_2O_3	6.5	4.7	8.0–9.5
%TiO_2	0.3	0.11	–
%Fe_2O_3	0.8	1.24	15.5–17.5
%MnO	3.3	< 0.1	< 0.2
%Na_2O	7.2	11.3	4.5–6.0[B]
%K_2O	0.1	0.31	
%F	5.9	9.4	8.5–10.0
%C_{Free}	1.5	4.5	–
CO_2	8.8	7.9	–
%C_{Total}	2.4	6.6	–
Loss on ignition	10.9	14.1	–
%H_2O	-	0.3	< 0.8
CaO/SiO_2	1.27	0.88	1.00–1.12
$(CaO + MgO)/(SiO_2 + Al_2O_3)$	1.07	0.82	–
Viscosity at 1300°C	1.1 Poise	2.51 Poise	–
Softening point (°C)	1000°C	1030°C	1080°C
Melting point (°C)	1110°C	1085°C	1130°C
Flowing point (°C)	1140°C	1145°C	1140°C

[A] The figures represent CaO + MgO (starting powder only)
[B] The figures represents N_2O+K_2O (starting powder only)

Laboratory studies

Laboratory studies carried out in the present work included measurements of physical properties such as apparent thermal diffusivity and surface tension. Thermal characterization of the powder was carried out by DSC measurement and the melting behaviour was further studied by simulating the melting of the powder in a laboratory furnace equipped with X-ray.

Thermal diffusivity measurement

The apparent thermal diffusivity was obtained by measurements in Laser flash equipment, TC-7000H/MELT Ulvac-Riko at elevated temperatures. The principle of the technique is to subject the top surface of the sample to a predefined laser pulse. The heat pulse transported through the material to the bottom surface of the substrate is monitored by a photovoltaic infrared detector and the signal is amplified. The apparent thermal diffusivity could be calculated using software based on the half time for temperature rise.

Solid samples of mould slag were prepared in order to control the amount of crystallization. This was achieved by annealing the quenched slag discs obtained after the pre-melting procedure described above. The machined discs of glassy/crystalline slag had a diameter of approximately 12 mm and a thickness between 1.5 and 2.5 mm. Solid samples where measured between room temperature and 500°C.

Measurement of the liquid slag samples were carried out by sandwiching the liquid samples between two Pt-crucibles ('three-layer cell' arrangement). Measurements were carried out for several sample thicknesses by controlling the distance between the two Pt-crucibles and the thermal diffusivities were computed by a differential method. The liquid measurements were carried out during the cooling cycle between the temperatures 1500 and 1300°C.

The method and procedures have been described more in depth elsewhere[2,3].

Surface tension measurement

Surface tension is measured by using sessile drop equipment. This is basically a controlled atmosphere high temperature furnace (supplied by Thermal Technology Inc., Model 1000-3500-FP20) equipped with X-ray equipment (Philips BV-26 imaging system). A full description of the equipment is presented elsewhere[4]. A small sample of the slag was melted on a well-defined steel surface inside the furnace. At experimental temperature, the liquid droplet was exposed to the X-ray beam and the shape of the droplet was captured by a CCD camera. The digitalized image of the droplet was further processed using image analysis software developed jointly by Carnegie Mellon University, USA, and the Royal Institute of Technology, Stockholm. The contact angles between the substrate and the surface, as well as the volume of the droplet, were evaluated. The surface tension of the sample could be evaluated from these results.

DSC measurement

Differential Scanning Calorimeter (DSC) equipment (NETZSCH STA 449C Jupiter®) was used for calorimetric studies. The DSC measurements were carried out on a small sample (30–45 mg) of unprepared commercial mould flux at a heating rate of 10°C/min. Sapphire (56 mg) was used as the reference material. The DSC measurements were performed in synthetic air, which allowed free carbon and other constituents to be oxidized, simulating the conditions during casting in industrial practice.

Melting simulations

The heating up and melting of a mould flux during continuous casting were simulated in specially designed laboratory equipment shown in Figure 2. An alumina tube of 30 mm inner diameter acted as the vessel containing liquid steel. Low alloy steel was heated by a water cooled copper induction coil. The power input was controlled manually and the steel temperature was measured using an optical pyrometer.

On top of the liquid steel, mould flux was added to a total depth of 110–120 mm. The same X-ray equipment used in the sessile drop experiments was employed to monitor the melting rate at predefined intervals of 20 or 30 s (depending upon the melting behaviour of the powder) by following the positions of Pt markers carefully placed on top of the powder bed.

The steel was melted and heated to a temperature of 1600°C. In order to avoid formation of a slag, the heating and melting of the steel were carried out in an alumina crucible provided with a lid. Further, a protective Ar atmosphere was used to flush through the system. At the experimental temperature, the induction unit power control was set to a predefined value in order to maintain a constant temperature during the runs.

The start of the experiment was marked by the removal of the protective lid and the first addition of mould flux powder. No temperature measurement was possible after the addition of mould flux. The mould flux powder was added continuously during the experiment in order to maintain a fixed bed height. No record was kept on the amount of flux added. Pt markers were placed on the bed top between the powder additions in order to visualize the bed movement on the X-ray images.

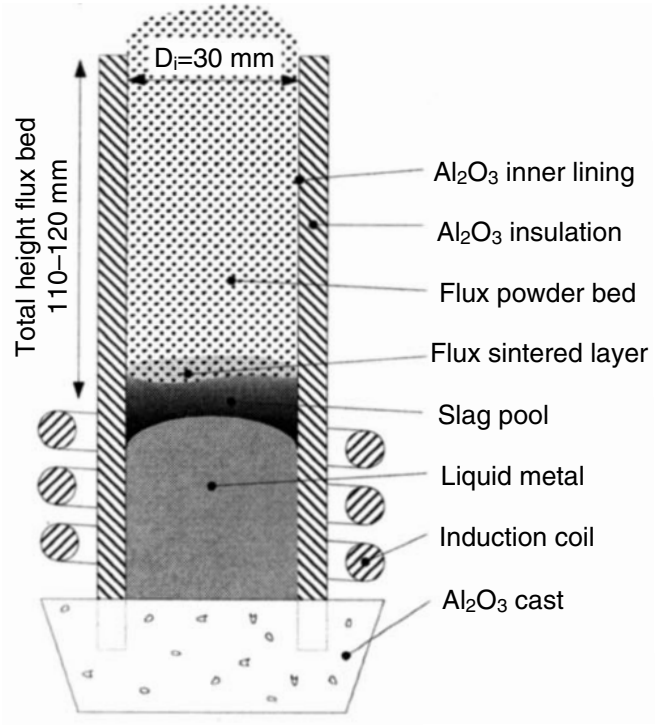

Figure 2. Illustration of the equipment used for mould flux powder melting simulation

The lowering of the positions of the Pt markers marked the sinking rates of the powder beds. This method enabled one to record the actual sinking rate of the central part of the flux bed, thus eliminating influence by wall effects such as sticking. The X-ray images also revealed, to some extent, differences in material density, thus enabling the distinct identification of powder and sintered and liquid layers.

Results and observations

DSC measurements

The results from DSC measurements on the two fluxes indicate that as the temperature is increased, several reactions take place. These are clearly detected in the graphs in Figure 3.

The initial exothermic peaks marked 'A' in the Figures, located at the temperature interval 180–310°C, are likely to be associated with the chemical reactions in the mould flux apart from the release of moisture. It is possible that the basic oxide components could form hydroxilic compounds if moisture release is hindered by the height of the powder bed.

Both samples show a major exothermic peak at just below 500°C, marked 'B' in the figures, which is associated with the combustion of carbon black particles added to the mould flux[5]. The next exothermic peak is present in only flux B, 'C' in Figure 3, at approximately 580°C. This could be associated with further combustion of carbonaceous materials, probably coke dust[5].

The following peak, marked 'D' in both plots, is endothermic and positioned slightly below 700°C, which is believed to reflect the decomposition of sodium carbonates. These peaks are slightly overlapped by the large exothermic peaks of carbon combustion and could therefore be difficult to detect.

Increasing the temperature further and the next exothermic peak is found in flux A at approximately 790°C, 'E' in Figure 3, which is likely to be associated with the combustion of graphite[5].

At higher temperatures, an endothermic peak was observed at approximately 900°C, 'F', in both samples. These peaks reflect the decomposition of calcium carbonates.

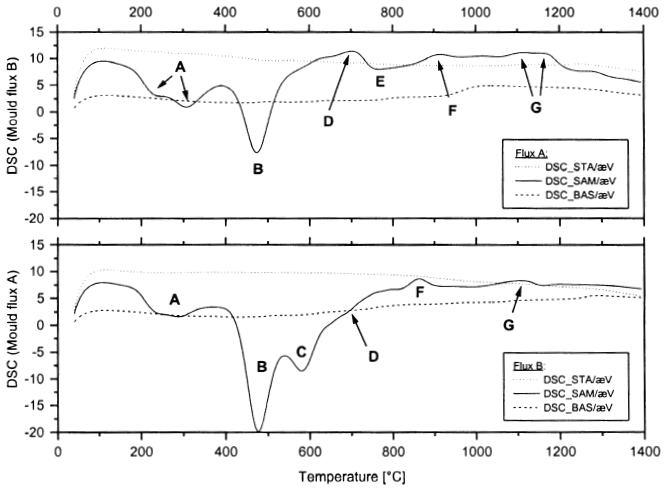

Figure 3. DSC graph mould flux A (top graph) and B (bottom graph)

As the temperature approaches 1100°C, both powders display endothermic peaks that represent the melting of the powder constituents ('G' in the Figure 3, DSC plots).

The powder melting

X-ray images of the flux melting simulation shows that there is a difference between the two mould flux beds' structures, as can be seen in Figure 4. Mould flux A shows a totally different bed structure from flux B. The cross-section, in this case, consists of only the loosely packed powder layer located directly on top of the liquid slag layer. Only a very thin sintered and/or semi-liquid layer could be detected in the figure.

Mould flux B is built up by a multi-layer structure with the loosely packed powder layer on top. This layer represents the major part of the total bed height. Below the powder layers, the sintered layer is present. This can be detected due to its slightly higher density observed in the X-ray images. It was also to some extent possible to identify the sintered layer due to the decrease in vertical movement of the Pt markers as they crossed the interface between the loosely packed and sintered layers. In Figure 5 this point is marked by arrows and is detected due to the decreased sinking rate relative to other Pt markers still positioned in the powder layer, i.e. the distance between the marker curves starts to narrow.

Underneath the sintered layer, flux B shows a semi-liquid layer. It is interesting to note the presence of metallic droplets in this two-phase layer. Observations during the experiments reveal that the metal drops are released from the bulk metal and transported through the liquid slag.

The two-phase layer is significantly absent in the case of flux A, as can be seen in Figures 4 and 5. This could be due to the specific characteristic of the powder, which results in very fast sinking of the flux bed. The sinking rate is almost constant throughout the bed thickness and shows no trace of any sintered layers.

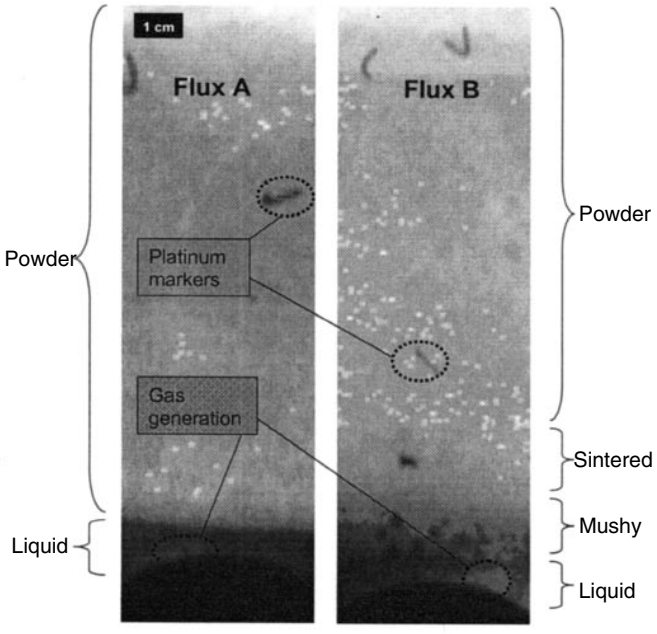

Figure 4. X-ray image showing the cross-section of the mould flux bed for flux A and B respectively during melting trials in laboratory equipment

Experimental observations showed that during the initial period of time after the addition of the mould flux on top of the free liquid iron surface, the gas evolution was strong. The gas at this initial stage is believed, due to the rapid raise in temperature, to consist of a mixture of all the gas components detected in the DSC measurement previously discussed. The agitation due to this was so vigorous that powder fluidization was observed. 15–45 s after the first powder addition had taken place, the gas evolution decreased rapidly and only local gas channelling could be observed. This corresponds approximately to the period of time necessary to form a liquid slag layer and the semi-steady-state to be established.

Thermal diffusivity and interfacial tension

The apparent thermal diffusivity was measured for the liquid mould flux slag at different temperatures, the results of which are presented in Figure 6. The two fluxes show slightly different values with a very small temperature dependency. The average apparent thermal diffusivity over the measured temperature interval is $3.72 \cdot 10^{-7}$ and $4.02 \cdot 10^{-7}$ m^2/s for flux A and B, respectively.

The surface tension measurement of the liquid slag showed that there is a small temperature dependency, but a relatively large difference between the two powders. The interfacial tension corresponding to flux B was measured to be 910 mN/m and the corresponding value for flux A was 1150 mNm, measured at 1322°C and 1178°C, respectively. The corresponding contact angles were 60° for flux A and 64° for flux B.

The liquid slag pool

Figure 7 shows the composition of the liquid slag pool as a function of casting time for the plant B casting sequence. Initially, the slag pool composition reflects the starting powder (high FeO content) but instantly starts to change towards the composition given by the addition of the production powder. After approximately 30 min, which represents approximately 50% of the first heat casting time, the effects of the starting powder on the liquid pool composition have disappeared.

It is generally believed that the slag pool should act as a chemically inert layer sealing off the liquid steel from the oxidizing atmosphere above. In the laboratory X-ray experiments, however, some gas generation at the slag-steel interface has been observed, as can be seen in Figure 4. This is likely to be due to the mould flux carbon reacting with oxygen dissolved in the steel.

Discussion and practical aspects

DSC discussion

The DSC measurement suggests that the difference in composition of the two powders, which can be seen in Table I, is not only due to a difference in mixing ratios, but also due to the use of different raw materials. This finding is most obvious when studying the carbon combustion peaks, which indicate that different types of carbon have been added to the mould flux.

The DSC plots also indicate that different mineral raw materials have been used, which is marked, to some extent, by the difference in the low temperature peaks ('A') as well as during melting ('G'), Figure 3.

The powder bed structure

The difference in melting rate between flux A and flux B is likely to be due to due to several reasons:

Carbon combustion

The carbon content, type and grain size are known to influence the melting rate[6]. The use of a 'high temperature carbon' such as graphite, which was used in flux A according to the DSC measurement result, separates the mineral grains in the powder for a longer period of time, even at higher temperatures. Thus, point-to-point contact is

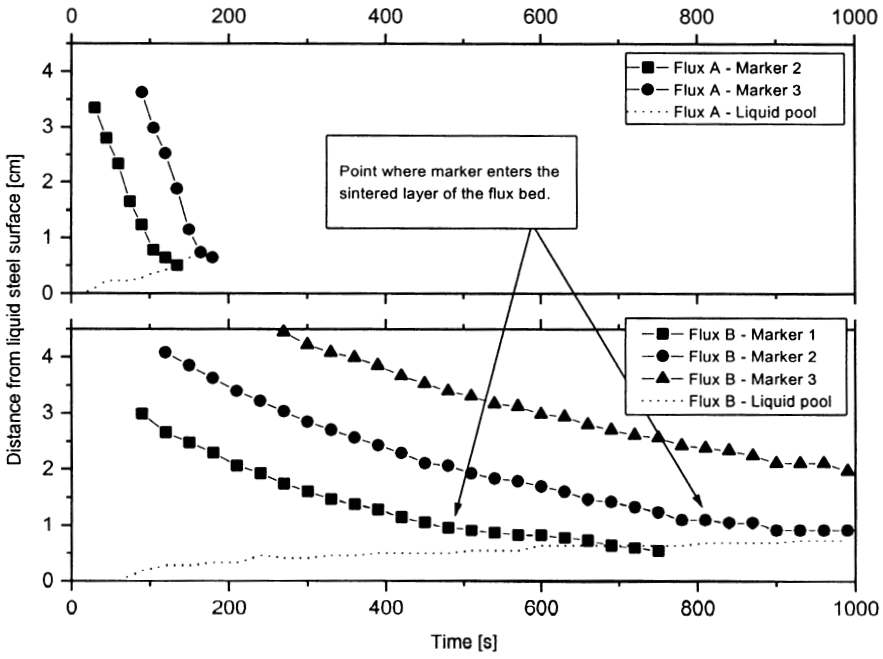

Figure 5. Plot showing the tracking of Pt tracers added to the mould flux in melting trials for flux A (upper graph) and B (lower graph). Pt markers are clearly visible in Figure 4

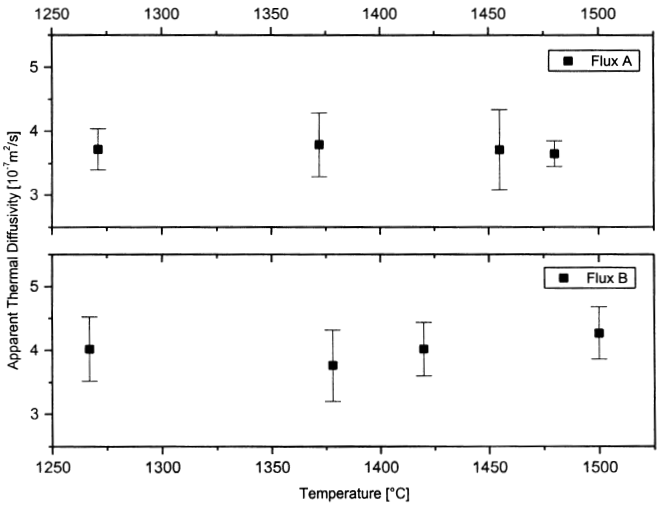

Figure 6. Apparent thermal diffusivity at some temperatures for the liquid slags of fluxes A and B

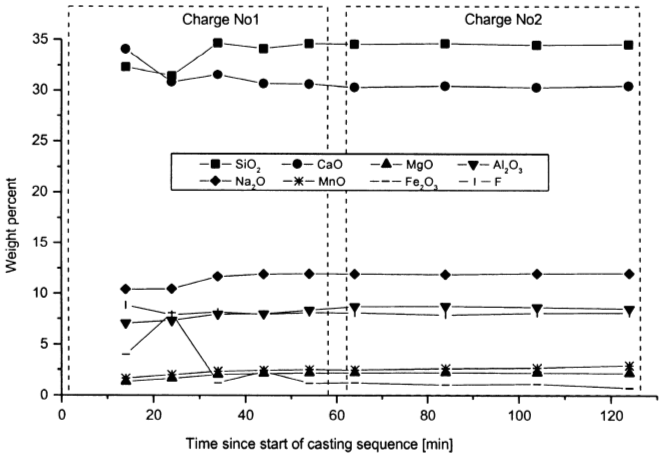

Figure 7. Liquid slag pool chemical composition vs. time during a two-sequence casting at plant B

not likely to exist during the main part of the heating up sequence. As the ignition temperature of the graphite finally is exceeded CO-gas is formed. If there is sufficient amount of oxygen available at this point, all carbon is likely to be removed and fusion can take place.

An increase in free carbon content is in general known to reduce the melting rate of a mould flux[6]. Flux B has considerably higher carbon content relative to flux A, Table I. This is likely to decrease the vertical heat transfer and the number of point-to-point contacts between the powder grains. When the temperature of flux B exceeds 750°C, most of the free carbon is likely to have been oxidized, leaving the flux grains surfaces uncovered. Point-to-point contact will then be established, which allows sintering and melting to take place.

If the available amount of oxygen is insufficient to oxidize all carbon, which might be the case at high carbon contents, some carbon might remain in the flux at elevated temperatures. It is believed that this carbon may be present in the sintered and mushy layer structure, slowing down the fusing rate further.

Length of melting interval

The absence of sintered and semi-solid layers during heating and melting in flux A indicates that the raw materials used have a composition forming liquid products at a short melting interval. If point-to-point contact is established at an early stage of the heating sequence, minerals may react to form low melting point products. These will, in turn, lead to the formation of two-phase layers at an earlier stage.

When studying the mould flux data sheet information (Table I), it is almost impossible to extract this difference in melting behaviour. In fact, the span between softening temperature and free flowing temperature is larger for fast melting powder A, indicating the opposite relationship. The temperature span between melting and free flowing, however, is considerably lower, which could be an indication of the short melting interval found during the melting experiments.

Drainage of formed liquid

Flux A also has a lower measured viscosity relative to flux B, as shown in Table I. This lower viscosity of flux A enables any formed slag liquid to drain away from the solid powder, thus avoiding any semi-solid region from being formed.

Melting rate

The melting rate of the powder is dependent on the overall thermal conduction of heat from the steel to the flux, through the liquid slag layer. Consequently, a higher heat transfer should result in a faster melting rate.

Approximate calculations of the heat flux were carried out in the two cases, assuming the same liquid pool thickness but different heat conduction and casting temperatures. By using the apparent thermal diffusivity measured in this study, as well as derived numbers from other studies[7], it is suggested that the difference in heat flux is not large enough to explain the difference in melting rate.

If the sink rate of the powder, based on the Pt markers shown in the X-ray measurements, is plotted as a function of liquid slag pool thickness, Figure 8, it is clear that these are related with a decrease in melting rate as the layer thickness increases. In practice, this means that the melting rate is to some extent self regulating in terms of controlling the liquid slag pool thickness.

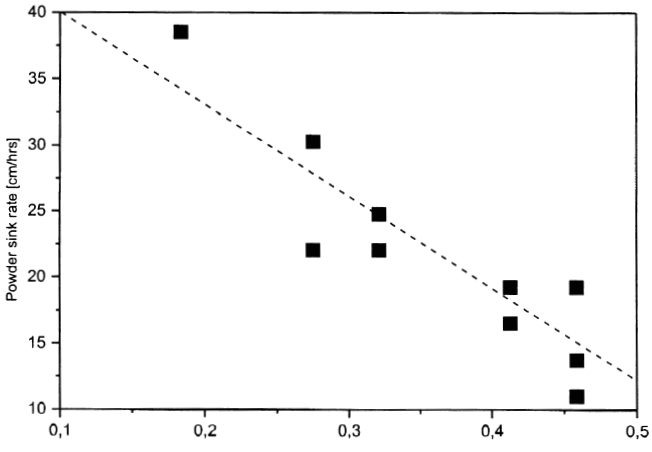

Figure 8. The sink rate of mould flux B as a functionof liquid pool depth

Table II
Mould flux functionality and properties relations

Flux	Designed property	Realized by	Achieved by	Side effects	Compensated by
Flux A	Soft cooling Fast melting rate	Crystalline phases in vertical layers Minimum solid state reaction or sintering. Short melting interval	High CaO/SiO_2-ratio Addition of high temperature carbon (graphite) Selection of flux minerals	Low viscosity of liquid None	Not a problem –
Flux B	Hard cooling Slow melting rate	Glassy phases in vertical layers Decreased vertical heat transfer	Low CaO/SiO_2-ratio Carbon addition	High viscosity of liquid, poor draining Prolonged heating leads to sintering and formation of solid solutions	Increased fluoride content.

When comparing the sinking rate from the x-ray experiments with the sinking rate of the powder bed in the casting operation, it is found that, in the production case, the rate is considerably higher, 2–4 times. When taking into consideration the larger liquid slag thickness in the production case, the difference is even bigger and somewhat surprising.

The effect could be due to the higher liquid steel area/cold wall ratio in the production case. Also, the mould oscillation may help to make the powder bed more compact, and break up any bridging that was sometimes observed during the laboratory experiments.

An alternative explanation is that the liquid slag layer is very thin in some parts of the steel-slag interface in a continuous caster. This is supported by two facts:

- Gas generation and mould flux sinks can usually be observed at a few local positions in the mould during casting, suggesting these areas represent zones with increased melting rate
- It is a well-known fact that the steel surface in the mould can form a non-linear shape, usually in the form of a standing wave, due to the fluid flow characteristics.

Slag pool chemical composition

The liquid slag pool is usually 15–20 mm thick in a production caster. If the density of the liquid slag is approximately 2.9 g/cm^3, the average residence time of the liquid flux on top of the liquid steel can be estimated by using the slab dimensions and flux consumption figures as input.

In the plant B case, 15–20 mm slag pool thickness corresponds to a 10–14 min period of time necessary to theoretically replace all the liquid slag with added fresh powder. The composition measurement as a function of time revealed this time to be considerably longer, 2–3 times longer, depending on the case, which of course, is likely to be due to the dilution effect. Regardless of how the calculation is performed, these figures emphasize the considerable length of time that the mould slag acts as a top slag.

If 30 minutes is taken as the average residence time of the slag, it means that 14–19 kg of liquid slag has been in contact with approximately 100 tons of liquid steel. Consequently, if only a very limited slag-metal interaction took place, one would expect that these reactions might affect the mould slag composition to a large extent, which in turn might influence the mould slag functionality.

Although the steel used at plant B was Al-killed, no clear effect of any slag-metal reactions could be detected. Figure 7 indicates an increase in Al_2O_3 content for almost the full time of the first heat, which is close to the earlier reported time necessary to obtain steady state[8], but the result is uncertain and somewhat interfered with by the starting powder addition. In addition, the amount of alumina pick-up in the slag pool in the clean steel casting operation is limited, previously reported to have been 2–3%[5,8].

Interfacial reactions

During the flux B melting experiments, numerous metallic droplets were entrapped in the semi-solid layer directly on top of the liquid slag layer. These droplets were visually observed as they detached from the liquid steel and moved upwards, despite the density differences, into the mushy zone where the droplets were trapped. In the case of flux A, metallic droplets could only occasionally be observed and, due to the absence of two-phase, highly viscous, regions, they always moved back into the steel phase.

The reason for the above detachment of metal droplets and their entering the slag phase is supported by the acute contact angles indicating wetting conditions. The two fluxes show a difference in the measured surface tension, with flux B 26 per cent higher than flux A (relative flux A). On the other hand, the viscosity has an opposite influence, contributing to the entrapment in the case of powder B. The situation is complicated by the gas generation, which was observed in the laboratory melting experiments as shown in Figure 4. This indicates the occurrence of a chemical reaction.

The observation of interfacial reactions lowering the surface tension is a critical parameter for the steel quality since this will increase the risk of slag entrapment into the steel. This is a problem of increasing significance when the expected increases in casting speed will be realized. Faster casting speeds means higher flow rates into the mould, i.e. higher steel turbulence.

Practical considerations

The two fluxes A and B are designed in order to handle two different casting cases with respect to the horizontal heat transfer in the mould. This heat transfer is to a large extent controlled by the solid slag layers formed on the mould copper face and the properties of these solid layers.

Flux A is used in casting stainless peritectic grades where a soft cooling is crucial in order to avoid surface defects. To obtain a lower heat transfer through the solid slag, crystalline phases should precipitate upon cooling. In the case of flux B, the situation is the opposite with the objective to achieve high horizontal thermal release through the solid slag layers. This is obtained by allowing a glassy phase to be formed upon cooling.

In order to fulfil the different tasks of the powders, the chemical composition must be modified to control the solidification, which explains the large difference in chemical composition of the two powders. These composition differences result in totally different performances during the melting of the powder, as observed in the present study. This is a likely to be a consequence of the flux thermal performance design. Thus, the melting behaviour is of secondary importance and sometimes will be set aside due to priorities in the flux thermal design, Table II.

Conclusions

In the present study, the different aspects of melting of mould fluxes in continuous casting are discussed using several measuring techniques.

An experimental technique has been developed in order to simulate the melting behaviour of a flux in the mould. The technique has been found to be useful for qualitative studies, and significant differences in the melting mechanism of two mould fluxes were detected. This was found to be a consequence of the difference in chemical composition, but unlikely to be detected by a study of the mould fluxes datasheets alone.

A cross-sectional view of different powders reveals that up to four different material layers may exist in the bed: loosely packed powder layer, sintered layer, semi-solid layer and liquid slag layer. The existence (height) of the two intermediate layers is dependent on several factors related to the flux composition. Factors like selected carbon type, melting intervals of components or intermediate products, and liquid phase viscosity are likely to influence the melting mechanism.

It is believed that the melting rate of the mould flux is dependent on the liquid slag layer thickness. Thus, in continuous casting operation the melting rate is likely to be non-uniform with position in mould due to the difference in liquid slag layer thickness.

Mould slag composition is found to be influenced by the starting powder for as long as 30 min, representing the major part of the first heat casting time. Any slag-metal reaction is likely to influence the liquid slag composition due to the very high slag/steel ratio.

Observations of gas formation indicate that interfacial reactions between the steel and slag take place.

Acknowledgement

The financial support from Ternkontoret (Swedish Steel Producers' Association) is gratefully acknowledged.

References

1. MILLS, K.C. and FOX, A.B. Review of mould flux performance and properties. *Proc. 4th European Coninuous. Casting Conf.*, Birmingham, U.K. The Inst. Mining, Minerals and Mining, 2002. vol. 1, pp. 345–359
2. WASEDA, Y., MASUDA, M., WATANABE, K., SHIBATA, H., OHTA, H., and NAKAJIMA, K. Thermal diffusivities of continuous casting powders for steel at high temperature. *High Temp. Mat. Processes*, vol. 13, no. 4. 1994. pp. 267–276.
3. ERIKSSON, R., HAYASHI, M., and SEETHARAMAN, S. Thermal diffusivity of some silicate melts. *Inter. J. Thermophys.*, vol. 24, 2003. p. 785.
4. JAKOBSSON, A., NASU, M., MANGWIRU, J., MILLS, K.C., and SEETHARAMAN, S. Interfacial tension effects on slag-metal reactions, *Phil. Trans. R. Soc*. London, vol. 356, 1998. pp. 995–1001.
5. BOMMARAJU, R. Optimum Selection and Application of Mould Fluxes for Carbon Steels. *Steelmaking Conf. Proc.,* Washinton D.C., U.S.A. Iron and Steel Society, Inc. 1991. vol. 74, pp. 131–146.
6. XIE, B., WU, J., and GAN, Y. Study on amount and scheme of carbon mixed in CC mold fluxes. *Steelmaking Conf. Proc.,* Washinton D.C., U.S.A. Iron and Steel Society, Inc. vol. 74, 1991. pp. 647–651.
7. SUNDH, J. Characterisation of heat transfer in the mould powder slags in terms of heat conduction and radiation. Research report IM-2003–530, Swedish Inst. Metals Research, 2003
8. BEZUIDENHOUT, G.A. and PISTORIUS, P.C. Effect of alumina pickup on mould flux viscosity in continuous slab casting. *Ironmaking and Steelmaking*, vol. 27, no. 5. 2000. pp. 387–39.